UNUSUAL INFRARED FLUORESCENCE IN $PrCl_3(Nd^{3+})$ CRYSTALS

F. Varsanyi
Bell Telephone Laboratories, Murray Hill, New Jersey
(Received 3 September 1963)

A very intense and sharp fluorescence line is observed at 2.54 μ when anhydrous praseodymium chloride containing a few tenths of a percent Nd^{3+} is illuminated with blackbody radiation. Excitation is so efficient that a small tungsten filament lamp operated at one-tenth or less power with the filament just noticeably glowing allows detailed studies of the line at very high spectral resolution. The linewidth is less than 0.2 of a wave number. The decay time is in the order of 50 milliseconds.

The excitation radiation is absorbed by praseodymium ions while the emission is identified as the $X_1 - Z_1$ fluorescence of Nd^{3+} (for notation see Table I). Under similar conditions[1] with Nd in the familiar $LaCl_3$ host, the corresponding fluorescence has not been detected. The favorable properties of the present system arise from the presence of two different rare earths in widely different concentrations and the effective energy transfer between them.

The excitation spectrum (the intensity of the 2.54-μ fluorescence monitored as a function of the excitation wavelength) is reproduced in Fig. 1.

Table I. Relevant levels of Pr^{3+} and Nd^{3+} around 2.5 μ.

	Identification	Energy (cm^{-1}) Magnetic splitting, $H \| C_3$ (Lorentz units) in $LaCl_3$	in $PrCl_3$
	$Pr^{3+}\ ^3H_6$ $\mu = 3$	4230.5[a]	4226.26[b]
		None	None
X_1	$Nd^{3+}\ ^4I_{13/2}$ $\mu = \pm 1/2$	3931.12[c]	3931.96[d]
		-10.24[c]	-10.33[d]
Z_1	$Nd^{3+}\ ^4I_{9/2}$ $\mu = \pm 5/2$	0	0
		- 3.996[e]	- 4.01[d]

[a]This is lowest line of $Pr^{3+}\ ^3H_6$ group, well separated from the other lines and the most likely to participate in the Pr-to-Nd energy transfer. Obtained in fluorescence, G. H. Dieke and R. Sarup, J. Chem. Phys. 29, 741 (1958).

[b]Direct infrared absorption measurement; line is weak due to being forbidden by both electric and magnetic dipole selection rules; it is not observable in the diluted crystal; it might be $^3H_5 + {}^3H_5$ ion-pair line, but that group is not well-known enough to ascertain this assignment.

[c]From infrared absorption; studies in fluorescence by E. H. Carlson, Johns Hopkins Spectroscopic Report No. 18, 1960 (unpublished), agree when assumption about G_2 upper state is changed.

[d]From infrared fluorescence X_1 to Z_1.

[e]From paramagnetic resonance [C. A. Hutchison and E. Wong, J. Chem. Phys. 29, 754 (1958)]; this splitting is used here to calibrate the magnetic field.

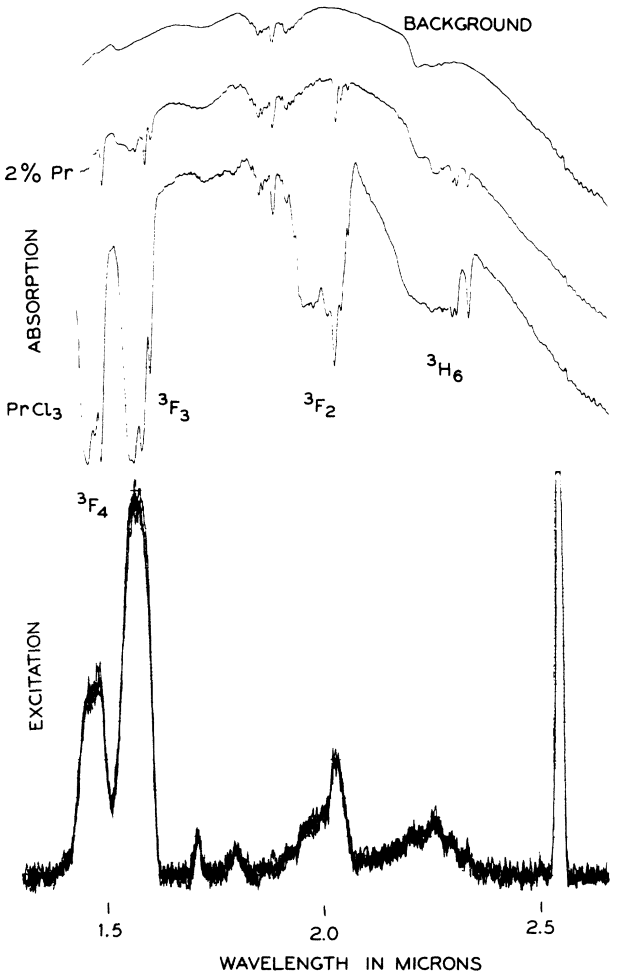

FIG. 1. Excitation spectrum of the 2.54-μ fluorescence compared to Pr absorption. All curves taken at 4°K. The excitation trace is a photographic superposition of four consecutive runs. (Tungsten lamp; one-meter grating monochromator scanning the wavelength range; sample; Fastie-Ebert 1.8-m spectrometer [Wm. G. Fastie, H. M. Crosswhite, and P. Gloersen, J. Opt. Soc. Am. 48, 106 (1958)] set at 2.54 μ; cooled PbS detector). The background curve combines the effects of the tungsten radiation, atmospheric absorption, efficiency of grating and optics, and detector sensitivity. (Tungsten lamp; one-meter grating monochromator; sample; PbS detector.) The 2% Pr is in $LaCl_3$.

Absorption traces also made with illuminating monochromator are shown for comparison, and the similarity to the excitation spectrum is easily recognized. Peaks at 2.54 μ and 1.69 μ are not due to fluorescence. There the wavelength of the excitation beam corresponds to wavelengths monitored by the detector spectrometer. All observations were made at liquid helium temperature. At higher temperatures the fluorescence intensity is gradually reduced and is absent at 77°K.

While there are substantial differences between the 100% $PrCl_3$ and 2% Pr in $LaCl_3$ traces, the general features are well preserved and the individual absorption groups are easily recognized. The dominant new feature in $PrCl_3$ is the strong absorption wing on the high-energy side of all groups. This agrees well with earlier observations on the visible part of the $PrCl_3$ spectrum.[2] The ion-pair excitation peaks observed then under modest resolution corresponded to the sum of the sharp $^3P_0$ metastable level and these broadened groups like $^3H_6$, etc., displayed in Fig. 1 here, while high-resolution[3] absorption measurements later showed the presence of many other ion-pair lines. Thinner sections of the $PrCl_3$ crystal reveal a fine structure of the broad side bands with dozens of relatively sharp lines. Detailed measurements are not yet available.

The lines of neodymium are somewhat shifted in $PrCl_3$ as compared to $LaCl_3$.[4] This would make the assignment of the extremely strong 2.54-μ line to Nd^{3+} just on the basis of near coincidence of wavelengths somewhat questionable. The Pr-like excitation spectrum makes additional confirmation even more desirable. The identification of the line is aided by high-resolution Zeeman experiments. As the internal electric field which acts on the Nd^{3+} ions is very nearly identical in the $PrCl_3$ and $LaCl_3$ lattices, the magnetic splitting factors for the corresponding levels are similar. This results in practically identical Zeeman patterns as illustrated in Fig. 2. Patterns in other orientations of the C_3 axis match similarly, including relative intensities and polarization.

The 50-msec decay and similar build-up times found here are unusually long but they do not necessarily require any special mechanism for explanation. Earlier measurements[5] of absolute oscillator strengths of several rare earths in $LaCl_3$ indicated values around 10^{-8} for the individual lines. Assuming similar values here one obtains a theoretical lifetime around 300 msec for the X_1 level. At this point one cannot say what portion of the buildup and decay is attributable to the Pr-to-Nd energy transfer process. Energy differences between the 4226-cm^{-1} praseodymium level and predicted[6] higher components of the $^3H_4$ ground state do fall in the range of the $^4I_{13/2}$ levels of neodymium. This points to the probable course of the energy transfer.

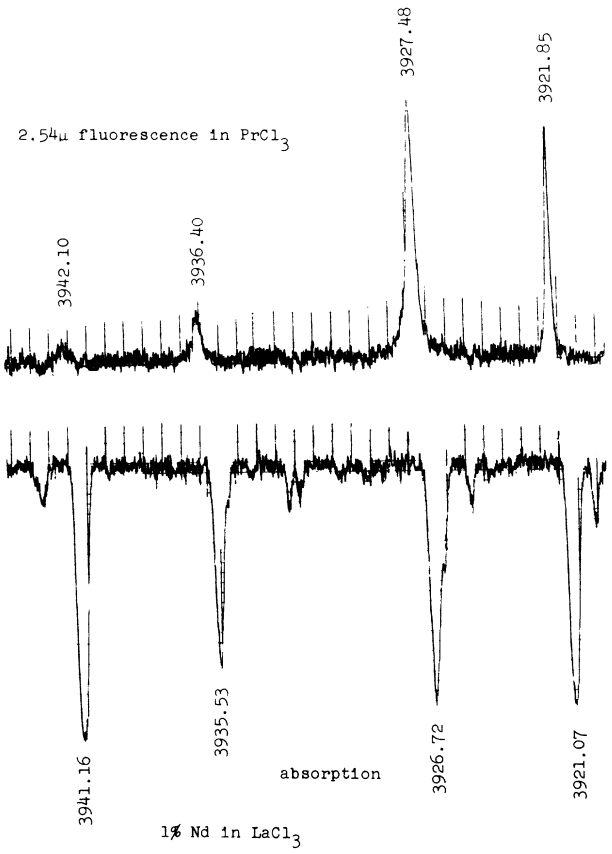

FIG. 2. Typical four-line Zeeman pattern of the 2.54-μ line. Magnetic field parallel to crystal C_3 axis. Field strength 30 240 gauss. The two high-energy lines in fluorescence are noticeably weakened indicating thermal equilibrium between upper-state components. Difference between $PrCl_3$ and $LaCl_3$ hosts is reflected in slight but noticeable shift of patterns. Wavelength markers are 5 Å apart. Numbers are in cm^{-1}. Unmarked lines belong to atmospheric water vapor. Resolving power is about 0.1 cm^{-1}. The fluorescence pattern was obtained by 4 watts total electrical power to the exciting tungsten lamp. $PrCl_3$ has 0.2% Nd^{3+}.

The author wishes to thank J. A. Burton for his enthusiastic support for building up the laboratory facilities which made the measurements possible, H. Guggenheim for his cooperation in growing the crystals used in this study, and B. Toth for his extensive experimental assistance.

[1]F. Varsanyi and G. H. Dieke, J. Chem. Phys. 33,

1616 (1960).
[2]F. Varsanyi and G. H. Dieke, Phys. Rev. Letters 7, 442 (1961).
[3]G. H. Dieke and E. Dorman, Phys. Rev. Letters 11, 17 (1963).
[4]Similar observations about Pr^{3+} levels were recently made by R. D. McLaughlin and J. G. Conway, J. Chem Phys. 38, 1037 (1963).
[5]F. Varsanyi and G. H. Dieke, J. Chem. Phys. 36, 835 (1962).
[6]B. R. Judd, Proc. Roy. Soc. (London) A241, 414 (1957).

THEORY OF THE PARALLEL FIELD MAGNETOACOUSTIC EFFECT

John J. Quinn*
Laboratories RCA Ltd., Zurich, Switzerland
(Received 19 July 1963)

Mackinnon, Taylor, and Daniel[1] have recently reported the observation of magnetoacoustic resonances in the attenuation of longitudinal sound waves propagating parallel to the magnetic field in cadmium. At present, no theoretical treatment[2-4] of this geometrical arrangement seems applicable to the experimental results. In fact, the semiclassical theory of Cohen, Harrison, and Harrison predicts that the attenuation should be completely independent of magnetic field. A possible explanation of the effect, based on rather intuitive reasoning, has been suggested by Mackinnon, Taylor, and Daniel. This explanation associates the effect with deviations from a spherical Fermi surface. The concepts involved are illustrated in Fig. 1, where the Fermi surface (or part of the Fermi surface) is taken to be an ellipsoid tilted at an angle away from the direction of the magnetic field $\vec{B}_0$. The effect of the field $\vec{B}_0$ is to cause electrons on the Fermi surface to move around the surface on a plane perpendicular to the direction of the field. The velocity of an electron in real space is normal to the Fermi surface. Thus electrons on the orbit marked *A* will oscillate back and forth in real space in the direction of $\vec{B}_0$ during each cyclotron period. Electrons on an orbit such as *B* will move a certain distance in the direction of $\vec{B}_0$ every cyclotron period. (The arrows indicate the direction of the velocity in real space at the points where they are drawn.) The possibility of spatial resonances between the wavelength of the sound wave and the "oscillation distance" in case *A* is obvious.

The object of this note is to present a fundamental theoretical treatment of this effect which points out the mathematical origin of the oscillations. A detailed analysis[5] of the dependence of the amplitude and period of the oscillations on the components of the effective-mass tensor, and on the detailed experimental conditions, will be presented elsewhere. The results obtained here confirm the qualitative picture suggested by Mackinnon, Taylor, and Daniel as the origin of the effect, although the detailed conditions for obtaining maxima and minima are somewhat different.

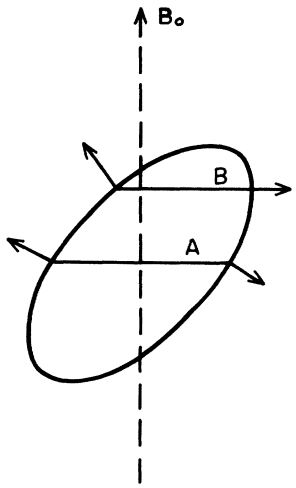

FIG. 1. A schematic of two possible electron orbits in k space in the presence of the field $\vec{B}_0$. In the case of orbit *A*, the electrons oscillate back and forth parallel to $\vec{B}_0$. This can easily be seen from the directions of the velocity in real space (normal to the constant energy surface) which are drawn at the ends of the orbit. The cross-sectional area of this orbit is a maximum, and we believe the resonances arise primarily from this orbit. In case *B*, the electrons will drift parallel to the magnetic field. They move with nonuniform velocity, but cover a given distance each cycle.

We start with the Hamiltonian H_0 for a single electron in the field B_0:

$$H_0 = \frac{1}{2m}\left\{\alpha_1 p_x^2 + \alpha_2\left(p_y - \frac{e}{c}B_0 x\right)^2 + \alpha_3 p_z^2 + \alpha_4\left[\left(p_y - \frac{e}{c}B_0 x\right)p_z + p_z\left(p_y - \frac{e}{c}B_0 x\right)\right]\right\}. \quad (1)$$